Optimal Nonlinear Estimation for Aircraft Flight Control in Wind Shear

Sandeep S. Mulgund* and Robert F. Stengel**
Department of Mechanical and Aerospace Engineering
Princeton University, Princeton, NJ 08544

Abstract

An Extended Kalman Filter (EKF) is developed to estimate the state of a jet transport aircraft. The EKF is based on the nonlinear longitudinal aircraft equations of motion, and it is designed to provide estimates of horizontal and vertical atmospheric wind inputs. The optimal state and disturbance estimates are incorporated in feedback control laws based on the aircraft's nonlinear inverse dynamics. The EKF produces accurate estimates, and the resultant flight trajectories are very similar to those obtained with perfect state feedback. The EKF is sensitive to uncertainty in the dynamic model, but much of the lost performance can be restored by treating the uncertainty as a random disturbance input.

Nomenclature

D	Drag
$E(\cdot)$	Expected value
E_s	Specific Energy
F	Nondimensional wind shear hazard index
g	Acceleration due to gravity
h	Altitude
I_{yy}	Moment of Inertia about body y-axis
L	Lift
m	mass
M	Pitching Moment
q	Pitch rate
r	Rate of climb
R	Radius of downdraft column
s	Laplace variable
t	Time
T	Engine Thrust
$\mathbf{u}$	Aircraft control vector
U_{max}	Maximum horizontal wind speed
V_a	Airspeed
w_x	Wind component along the x-axis
w_h	Wind component along the h-axis
W	Weight
x	Distance along x-axis
$\mathbf{x}$	Aircraft state vector
$\mathbf{y}$	Control system command vector
z_{max}	Altitude of maximum outflow
α	Angle of attack
γ	Flight Path Angle
δ_E	Elevator deflection
δ_T	Throttle setting
θ	Pitch Attitude

Superscripts

$(\dot{})$	Time derivative
$(\hat{})$	Estimated quantity

Subscripts

a, A	Air-mass-referenced quantity
c	Commanded value
i, I	Inertially referenced quantity

Introduction

Severe low-altitude wind variability represents an infrequent but significant hazard to aircraft taking off or landing. During the period from 1964 to 1985, *microburst wind shear* was a contributing factor in at least 26 civil aviation accidents involving nearly 500 fatalities and over 200 injuries [1]. A microburst is a strong localized downdraft that strikes the ground, creating winds that diverge radially from the impact point. The effects of microburst wind shear on airplane dynamics have only recently been understood in detail, and it has been found that effective recovery from inadvertent encounters may require counterintuitive piloting techniques [2].

The aviation community has initiated an extensive research effort to solve the wind shear problem. The Federal Aviation Administration (FAA) and the National Aeronautics and Space Administration have established an integrated program to address the wind shear problem through focused research and development programs [3,4]. The FAA's *Wind Shear Training Aid* [5] recommends that on recognizing an encounter with severe wind shear, the pilot should command maximum thrust and rotate the aircraft to an initial target pitch angle of 15°. This pitch target was identified through rigorous analyses using full six-degree-of-freedom flight simulators and wind models representative of actual accident cases [6].

Optimal trajectory analysis (OTA) has been used to identify the limits of aircraft performance in wind shear and to determine the control strategies required to achieve such performance [7-13]. Computation of these trajectories requires global knowledge of the flow field. Since this is not possible in practice, OTA results are not

* Currently Senior Scientist, Charles River Analytics Inc., Cambridge, MA.

** Professor

Presented at the 19th ICAS Congress, Anaheim, CA, Sept. 1994

immediately useful for real-time aircraft control. Consequently, feedback control laws employing local wind-field knowledge have been developed for near-optimal flight control [7, 14-16].

The goal of this research is to bridge the gap between the performance achieved using OTA and that attainable using feedback control based on local (and possibly forward-look) wind field knowledge. In a recent paper [17] we presented the design of a feedback control law based on the aircraft's *nonlinear inverse dynamics* (NID) [18-23]. The NID controller demonstrated safe flight through severe microbursts encountered on the final approach. It was assumed that the aircraft state was known exactly, as were horizontal and vertical wind inputs. The issue of estimating the aircraft state and disturbance inputs from available sensor outputs is the focus of this paper. The Extended Kalman Filter (EKF) is postulated as a suitable estimator structure, and it is evaluated in concert with the NID control laws.

Effect of Wind Shear on Airplane Dynamics

Aircraft Model and Equations of Motion

A three degree-of-freedom model of a twin-jet transport aircraft is used for this study. The aircraft has a gross weight of 85,000 lb and maximum takeoff thrust of 24,000 lb. Its aerodynamic coefficients are complex nonlinear functions of altitude, Mach number, incidence angles, rotation rates, control deflections, configuration changes (such as gear and flap deflection), and ground proximity. Effects of wind shear on aircraft motion and aerodynamics are modeled using the technique described in [24, 25]. The relevant reference frames used to describe the aircraft's position, orientation, and velocity are presented in Fig. 1. Flight is assumed to take place in a vertical plane over a flat Earth, and a coordinate system fixed to the ground is defined as the inertial reference frame. On the basis of these assumptions, the equations of motion are:

$$\dot{x} = V_a \cos\gamma_a + w_x \tag{1}$$

$$\dot{h} = V_a \sin\gamma_a + w_h \tag{2}$$

$$\dot{V}_a = \frac{T}{m}\cos\alpha_a - \frac{D}{m} - g\sin\gamma_a - \dot{w}_x\cos\gamma_a - \dot{w}_h\sin\gamma_a \tag{3}$$

$$\dot{\gamma}_a = \frac{1}{V_a}\left(\frac{T}{m}\sin\alpha_a + \frac{L}{m} - g\cos\gamma_a - \dot{w}_h\cos\gamma_a + \dot{w}_x\sin\gamma_a\right) \tag{4}$$

$$\dot{\alpha}_a = q - \dot{\gamma}_a \tag{5}$$

$$I_{yy}\dot{q} = M \tag{6}$$

The effect of wind shear on airplane energy state can be described compactly. First define the specific energy (energy per unit weight) as the sum of air-mass relative kinetic energy and inertial potential energy:

$$E_s = \frac{V_a^2}{2g} + h \tag{7}$$

Differentiating this expression and substituting from eqs. 1-3,

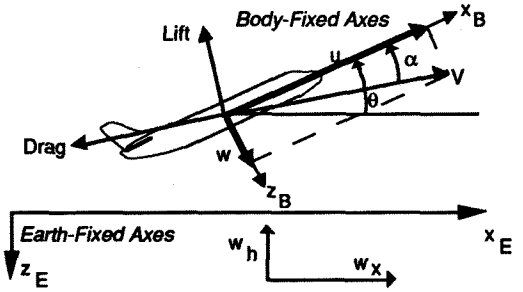

Figure 1. Coordinate Systems and Reference Frames.

$$\dot{E}_s = V_a\left(\frac{T\cos\alpha_a - D}{W} - \frac{\dot{w}_x}{g}\cos\gamma_a - \frac{\dot{w}_h}{g}\sin\gamma_a + \frac{w_h}{V_a}\right) \tag{8}$$

The first term is recognizable as the airplane's specific excess power. The three wind terms describe wind shear impact on airplane energy state, and they may be combined into a single scalar quantity called the "F-Factor" [3] as follows:

$$F = \frac{\dot{w}_x}{g}\cos\gamma_a + \frac{\dot{w}_h}{g}\sin\gamma_a - \frac{w_h}{V_a} \tag{9}$$

The vertical shear term is typically quite small and often neglected. The effect of wind shear on airplane performance is thus expressed as an effective reduction in available specific excess power due to horizontal and vertical shears and downdrafts. Regions where F is negative are considered to be *performance-increasing* shears, while regions where F is positive are *performance-decreasing*. F values of more than 0.15 cancel the climb gradient capability of most jet transports.

The aircraft's lift, drag, pitching moment and thrust are expressed as,

$$L = \bar{q}S_{ref}C_L \tag{10}$$

$$D = \bar{q}S_{ref}C_D \tag{11}$$

$$T = T_{max}(V_a)\delta_T \qquad 0 \le \delta_T \le 1 \tag{12}$$

$$M = \bar{q}S_{ref}\bar{c}C_M \tag{13}$$

The wind components and spatial gradients used in the equations of motion are obtained from the Oseguera-Bowles downburst model [26]. This analytic time-invariant model represents an axisymmetric stagnation point flow, and it permits simulation of microbursts of varying size and strength through specification of the radius of the downdraft column, the maximum outflow, and the altitude of maximum outflow.

Nonlinear Flight Control

This description of nonlinear control methods is necessarily brief. More complete treatments can be found in [27, 28]. The following derivation is from [29]. Given a system of the form,

$$\dot{\mathbf{x}} = \mathbf{f}(\mathbf{x}) + \mathbf{G}(\mathbf{x})\mathbf{u} \tag{14}$$

where $\mathbf{x}$ is n x 1 and $\mathbf{u}$ is m x 1, we define an m-dimensional output vector,

$$\mathbf{y} = \mathbf{H}(\mathbf{x}) \tag{15}$$

It is possible to construct a nonlinear feedback control law that provides output decoupling of the elements of $\mathbf{y}$ or their derivatives such that $\mathbf{y}^{(d)} = \mathbf{v}$. The new control input $\mathbf{v}$ can be chosen to place the system poles in desired locations (for example, to achieve desired specifications on response overshoot and settling time). The vector $\mathbf{y}^{(d)}$ is expressed as,

$$\mathbf{y}^{(d)} = \mathbf{f}^*(\mathbf{x}) + \mathbf{G}^*(\mathbf{x})\mathbf{u} = \mathbf{v} \tag{16}$$

and d is the *relative degree of differentiation* required to identify a direct control effect on each element of the output vector. The inverse control law then is

$$\mathbf{u} = [\mathbf{G}^*(\mathbf{x})]^{-1}[\mathbf{v} - \mathbf{f}^*(\mathbf{x})] \tag{17}$$

and the closed-loop dynamics of the system take the form,

$$\dot{\mathbf{x}} = \mathbf{f}(\mathbf{x}) + \mathbf{G}(\mathbf{x})[\mathbf{G}^*(\mathbf{x})]^{-1}[\mathbf{v} - \mathbf{f}^*(\mathbf{x})] \tag{18}$$

While the expression of the inverse control law appears simple, its implementation can be quite complex. Evaluation of the functions $\mathbf{f}^*(\mathbf{x})$ and $\mathbf{G}^*(\mathbf{x})$ requires that a full, d-differentiable model of the aircraft dynamics be included in the control system. The controller can be simplified if the system can be partitioned into slow and fast-time-scale subsystems [30]. The separation of the dynamics into fast and slow time-scales is a natural consequence of the underlying physics. For the aircraft problem, it is assumed that the pitch rate evolves faster than the flight path and velocity. This is consistent with the time-scale separation between the phugoid and short-period modes of an aircraft's longitudinal dynamics [31]. This technique has been applied to the flight control problem [17, 19 -23]. In the present study, the effects of wind shear are explicitly considered in the inversion.

Three sets of output vectors are considered for approach encounters with wind shear: airspeed/climb rate, groundspeed/climb rate, and throttle/climb rate [17]. A combination of airspeed, groundspeed, and climb-rate regulation [32] is employed during glide slope tracking on the final approach. When the wind shear F-Factor (eq. 9) exceeds a certain threshold, the controller commands an aborted-landing maneuver using full throttle and a nominal positive climb rate. The controller demonstrates good recovery performance in a variety of microburst encounters when perfect state feedback is used as the basis of the control. Such full-state feedback would not be available in practice – it would be necessary to estimate the aircraft state and disturbance components from noisy sensor outputs. An Extended Kalman Filter has been developed to accomplish this task, and it is now described.

Optimal State Estimation

An optimal estimator is a computation algorithm that processes measurements to calculate a minimum-error estimate (in accordance with some stated optimality criterion) of the state of a dynamic system using [33]:

- Knowledge of system and measurement dynamics
- Assumed statistics of system disturbance inputs and measurement errors
- Initial condition information

Such an algorithm minimizes estimation error in some well-defined statistical manner and makes use of all of the measurement data and prior knowledge about the system. However, its potential drawback is sensitivity to erroneous system models and statistics. The Extended Kalman Filter derives optimal aircraft state and wind component estimates for use with the NID control laws. The EKF is an optimal filter in the sense that it minimizes the variance in the estimation error associated with a nonlinear system's linear perturbation model.

The Extended Kalman Filter computes minimum-variance estimates for nonlinear systems described by the ordinary differential equation

$$\dot{\mathbf{x}}(t) = \mathbf{f}[\mathbf{x}(t), \mathbf{u}(t), t] + \mathbf{w}(t) \tag{19}$$

The vector $\mathbf{f}$ is a nonlinear function of the state $\mathbf{x}$, the deterministic control input $\mathbf{u}$, and time. The disturbance input $\mathbf{w}$ is a white, zero-mean Gaussian random process:

$$E[\mathbf{w}(t)] = \mathbf{0} \tag{20}$$

$$E\left[\mathbf{w}(t)\mathbf{w}^T(\tau)\right] = \mathbf{Q}_c(t)\delta(t-\tau) \tag{21}$$

where $E(.)$ denotes the expected value of the function. The disturbance is thus characterized by its spectral density matrix $\mathbf{Q}_c(t)$. The quantity δ is the Dirac delta function:

$$\delta(t-\tau) = \begin{cases} \infty & t = \tau \\ 0 & t \neq \tau \end{cases} \tag{22}$$

$$\lim_{\varepsilon \to 0} \int_{t-\varepsilon}^{t+\varepsilon} \delta(t-\tau)d\tau = 1 \tag{23}$$

Both continuous-time and discrete time measurements can be handled; considered here is the case of discrete measurements of the form

$$\mathbf{z}(t_k) = \mathbf{h}[\mathbf{x}(t_k)] + \mathbf{n}_k \quad k = 0, 1, 2, \ldots \tag{24}$$

The measurement noise $\mathbf{n}$ also is assumed to be a white, zero-mean Gaussian random process that is uncorrelated with the disturbance input:

$$E(\mathbf{n}_k) = \mathbf{0} \tag{25}$$

$$E\left(\mathbf{n}_k\mathbf{n}_k^T\right) = \mathbf{R}_k \tag{26}$$

$$E\left[\mathbf{w}(t)\mathbf{n}_k^T\right] = \mathbf{0} \text{ for all } k \text{ and all } t \tag{27}$$

The expected values of the initial state and its covariance are assumed known:

$$E(\mathbf{x}_0) = \hat{\mathbf{x}}_0 \tag{28}$$

$$E\left[(\mathbf{x}_0 - \hat{\mathbf{x}}_0)(\mathbf{x}_0 - \hat{\mathbf{x}}_0)^T\right] = \mathbf{P}_o \tag{29}$$

Before presenting the equations for the computation of the state estimate and its covariance, it is necessary to define the sensitivity matrices:

$$\mathbf{F}(t) = \mathbf{F}[\mathbf{x}(t), \mathbf{u}(t), t] \equiv \left.\frac{\partial \mathbf{f}[\cdot]}{\partial \mathbf{x}}\right|_{\mathbf{x}(t)=\hat{\mathbf{x}}(t)} \tag{30}$$

$$\mathbf{H}(t) = \mathbf{H}[\mathbf{x}(t)] \equiv \left.\frac{\partial \mathbf{h}[\cdot]}{\partial \mathbf{x}}\right|_{\mathbf{x}(t)=\hat{\mathbf{x}}(t)} \tag{31}$$

The EKF propagates (or *extrapolates*) both the state estimate and its covariance using the system model. New measurements are combined with the extrapolated estimate to generate an "updated" estimate. The state covariance also is updated to reflect the information contained in the measurement. A weighting factor called the Kalman Filter gain is used to combine the extrapolated estimate with the new measurement. This gain is defined in such a way that it minimizes the estimation error covariance after the update. It is useful to introduce notation that distinguishes state estimates made before and after the measurement updates: $\hat{\mathbf{x}}_k(-)$ is the state estimate resulting from extrapolation alone (i.e., before the observation $\mathbf{z}_k$ is considered), and $\hat{\mathbf{x}}_k(+)$ is the corrected estimate that accounts for the measurements. The pre- and post-measurement covariance matrices $\mathbf{P}_k(-)$ and $\mathbf{P}_k(+)$ are defined similarly. The state and covariance estimates are extrapolated using

$$\hat{\mathbf{x}}[t_k(-)] = \hat{\mathbf{x}}[t_{k-1}(+)] + \int_{t_{k-1}}^{t_k} \mathbf{f}\{\hat{\mathbf{x}}[\tau(-)], \mathbf{u}(\tau), \tau\} d\tau \tag{32}$$

$$\mathbf{P}[t_k(-)] = \mathbf{P}[t_{k-1}(+)] + \int_{t_{k-1}}^{t_k} \left[\mathbf{F}(\tau)\mathbf{P}(\tau) + \mathbf{P}(\tau)\mathbf{F}(\tau)^T + \mathbf{Q}_c(\tau)\right] d\tau \tag{33}$$

The *Jacobian* $\mathbf{F}(\tau)$ is evaluated in the interval for corresponding values of $\hat{\mathbf{x}}[\tau(-)]$. The state and covariance are updated as

$$\hat{\mathbf{x}}_k[t_k(+)] = \hat{\mathbf{x}}_k[t_k(-)] + \mathbf{K}(t_k)\left\{\mathbf{z}(t_k) - \mathbf{h}\left[\hat{\mathbf{x}}[t_k(-)]\right]\right\} \tag{34}$$

$$\mathbf{P}_k[t_k(+)] = \{\mathbf{I}_n - \mathbf{K}(t_k)\mathbf{H}(t_k)\}\mathbf{P}[t_k(-)] \tag{35}$$

The filter gain $\mathbf{K}(t_k)$ is

$$\mathbf{K}(t_k) = \mathbf{P}[t_k(-)]\mathbf{H}^T(t_k)\left\{\mathbf{H}(t_k)\mathbf{P}[t_k(-)]\mathbf{H}^T(t_k) + \mathbf{R}(t_k)\right\}^{-1} \tag{36}$$

The matrix $\mathbf{H}(t_k)$ is evaluated using $\mathbf{x} = \hat{\mathbf{x}}[t_k(-)]$. Equations 30 - 36 constitute the EKF algorithm for continuous-time nonlinear systems with discrete measurements.

Filter Equations for the Jet Transport

The EKF estimates the state of the jet transport aircraft using available inertial and air-data measurements. A key feature of the EKF in this application is its ability to estimate the horizontal and vertical wind components w_x and w_h, along with their first and second time-derivatives. Estimates of these quantities are used as the basis of feedback control using the NID control laws. Before presenting the EKF equations for the jet transport, it is worthwhile to briefly examine conventional methods of in-flight wind disturbance estimation.

The Federal Aviation Administration has stipulated that all commercial aircraft be outfitted with reactive wind shear detection systems by December, 1993. Typically, these systems compute an estimate of the F-Factor by differencing inertial and air-relative acceleration signals [34, 35], since any difference between air-relative and inertial acceleration must be due to unsteady motion of the airmass itself. An algorithm developed by Oseguera and Bowles [36] is based on a three-dimensional expression of the F-Factor, and it provides good estimates of F in many different flight conditions. This algorithm has become a measurement standard for the evaluation of forward-looking wind shear detectors. However, this method is not suitable for use with the NID control laws developed in this paper, as it does not derive w_x, w_h, and their first two time-derivatives from the F estimate.

Bossi and Bryson [37] examined the use of *constant-gain* Kalman Filters for disturbance estimation and detection of engine failure for a short-takeoff and landing (STOL) aircraft during the landing maneuver. The estimator is based upon a linearized model of open-loop aircraft dynamics, and their results suggest that it is possible to develop accurate estimates of horizontal and vertical winds (along with their first time-derivatives) by defining w_x, w_h, $\dot{w}_x$ and $\dot{w}_h$ as state elements and including them in the filter. This is the approach taken in the design of an EKF for the jet transport.

The wind-axis equations of motion (eqs. 1 - 6) are used to define the plant model for the estimator equations. There is a first-order lag in powerplant dynamics:

$$\dot{T} = \frac{T_c - T}{\tau} \tag{37}$$

where T_c is the commanded thrust, T is the actual thrust, and τ = 2 sec. The aircraft state vector is defined nominally as

$$\mathbf{x}_{ac}^T = [x \quad h \quad V_a \quad \gamma_a \quad \alpha_a \quad q \quad T] \tag{38}$$

The control input to the system is

$$\mathbf{u} = \begin{bmatrix} T_c \\ \delta_E \end{bmatrix} \tag{39}$$

The NID control laws also require feedback of w_x, w_h, $\dot{w}_x$, $\dot{w}_h$, $\ddot{w}_x$, and $\ddot{w}_h$. It is necessary to make these six variables part of the system state vector. The "wind state" vector is defined as

$$\mathbf{x}_d^T = [w_x \quad w_h \quad \dot{w}_x \quad \dot{w}_h \quad \ddot{w}_x \quad \ddot{w}_h] \tag{40}$$

In order to construct the system model, it is necessary to define the "dynamics" associated with the wind inputs. Any mathematical model of the wind dynamics represents an approximation to the conditions that exist within a microburst. Error in the modeling can lead to biases in the estimates and even divergence from the actual values. The simplest approach is to use an *integral-state* model [37] to represent the wind components and their time-derivatives. The equation describing the wind dynamics is

$$\dot{\mathbf{x}}_d = \mathbf{F}_d\mathbf{x}_d + \mathbf{w} \tag{41}$$

where

$$\mathbf{F}_d = \begin{bmatrix} 0 & 0 & 1 & 0 & 0 & 0 \\ 0 & 0 & 0 & 1 & 0 & 0 \\ 0 & 0 & 0 & 0 & 1 & 0 \\ 0 & 0 & 0 & 0 & 0 & 1 \\ 0 & 0 & 0 & 0 & 0 & 0 \\ 0 & 0 & 0 & 0 & 0 & 0 \end{bmatrix}, \quad \mathbf{w} = \begin{bmatrix} 0 \\ 0 \\ 0 \\ 0 \\ w_1 \\ w_2 \end{bmatrix} \qquad (42a, b)$$

and $\mathbf{w}$ is (by assumption) a white, zero-mean Gaussian random variable:

$$E[\mathbf{w}(t)] = \mathbf{0} \qquad (43)$$

$$E\left[\mathbf{w}(t)\mathbf{w}^T(\tau)\right] = \mathbf{Q}_c(t)\delta(t-\tau) \qquad (44)$$

The aircraft dynamics may thus be expressed as

$$\dot{\mathbf{x}}_{ac} = \mathbf{f}(\mathbf{x}_{ac}, \mathbf{u}, \mathbf{x}_d) \qquad (45)$$

where the elements of $\mathbf{f}(\cdot)$ are constructed using eqs. 1 - 6. The complete state vector for the estimator plant model is defined as

$$\chi \stackrel{\Delta}{=} \begin{bmatrix} \mathbf{x}_{ac} \\ \mathbf{x}_d \end{bmatrix} \qquad (46)$$

The combined aircraft/disturbance dynamics are then written as

$$\dot{\chi} = \begin{bmatrix} \dot{\mathbf{x}}_{ac} \\ \dot{\mathbf{x}}_d \end{bmatrix} = \begin{bmatrix} \mathbf{f}(\mathbf{x}_{ac}, \mathbf{u}, \mathbf{x}_d) \\ \mathbf{F}_d\mathbf{x}_d \end{bmatrix} + \begin{bmatrix} \mathbf{0} \\ \mathbf{w} \end{bmatrix} \qquad (47)$$

Equation 47 describes the assumed system model used to propagate the EKF. The disturbance input to this system is the vector $\mathbf{w}$, whose nonzero components physically represent the third time-derivatives of w_x and w_h. Thus, for the purposes of the EKF, $\dddot{w}_x$ and $\dddot{w}_h$ are *modeled* as zero-mean Gaussian random variables. There is a question of how to choose the elements of the matrix $\mathbf{Q}_c$ (eq. 44). Empirical data on microbursts generally include information on wind speeds, spatial extent and (possibly) F-Factor; it is difficult to infer anything substantive about the third time-derivative of the wind speed components. Consequently, it has been necessary to rely on trial-and-error methods to identify suitable elements of $\mathbf{Q}_c$. In effect, its components become design parameters that are adjusted to tune the filter's response. The numerical values used are presented along with the simulation results.

The measurement vector $\mathbf{z}$ consists of the sensor outputs that are available on a typical modern jet transport aircraft. These are altitude (ft), groundspeed (ft/sec), airspeed (ft/sec), angle of attack (deg), pitch angle (deg) and rate (deg/sec), altitude rate (ft/sec), and horizontal and vertical acceleration (ft/sec^2). The vector $\mathbf{z}$ is thus defined as

$$\mathbf{z}^T = \begin{bmatrix} h & V_i & V_a & \alpha_a & \theta & q & \dot{h} & \ddot{x} & \ddot{h} \end{bmatrix} \qquad (48)$$

The measurement noise covariance matrix is defined as

$$\mathbf{R} = \text{diag}(5^2, 3.6^2, 1.7^2, .5^2, .05^2, .05^2, .5^2, .322^2, .322^2) \qquad (49)$$

These values are representative of state-of-the-art inertial and air-data systems.

The EKF is now evaluated in conjunction with the NID control laws. The EKF/NID performance is compared to that achieved using perfect state feedback. This permits an assessment of how much performance is "lost" when optimal state estimates based on noisy measurements are used as the basis for the feedback.

Simulation Results

Aircraft encounters with microburst wind shear are considered on the final approach, during which a decision is made to abort the landing and execute a climb-out. A climb rate scheduling strategy [2] is used to compute the target climb rate during the aborted-landing maneuver as a function of available performance. This produces trajectories that exchange altitude for airspeed in a manner dependent on microburst strength, similar to previously obtained trajectory optimization results [13].

The disturbance input spectral density matrix $\mathbf{Q}_c$ is set to

$$\mathbf{Q}_c = diag(0,0,0,0,0.01,0.01) \qquad (50)$$

The zero off-diagonal components imply that the horizontal and vertical wind inputs are uncorrelated with one another. The nonzero diagonal elements were determined through trial-and-error. If they were made too large, the EKF did a poor job of attenuating measurement noise in its derivation of state and disturbance estimates. Very small diagonal elements resulted in good measurement noise attenuation but introduced significant lags into the estimates of many of the state components. This estimator lag led to degraded controller performance. Numerical instabilities also were encountered in the propagation of the state and covariance estimates when small numbers were used as the diagonal elements of $\mathbf{Q}_c$. The selected numbers provide a good balance between attenuating measurement noise and minimizing estimator lag.

The simulation results are organized to facilitate a comparison of the EKF/NID flight trajectory with that obtained using perfect state feedback, and to illustrate the estimation performance of the EKF. State estimation *errors* are shown together with the "2σ" error estimate, which is computed from the covariance matrix $\mathbf{P}(t)$. The $\pm 2\hat{\sigma}_i(t)$ curves provide the estimated 95% confidence interval on the error associated with the state estimate $\hat{\chi}_i(t)$. The aircraft is initialized on the glide slope at a point well outside the microburst core with an initial groundspeed of 245 ft/sec. The microburst has a core radius of 3,000 ft, a maximum horizontal wind speed of 70 ft/sec, and a maximum outflow altitude of 150 ft. The controller initiates the aborted-landing maneuver once the estimate of the F-Factor exceeds a threshold of 0.075. The initial state estimate is set equal to the actual state, so that $\hat{\chi}(t_o) = \chi(t_o)$. The covariance matrix is initialized as an identity matrix of appropriate dimension.

Figures 2 and 3 present airspeed and angle of attack vs. range from microburst core in both the NID-only and the EKF/NID trajectories. Figure 4 shows the horizontal and vertical wind components experienced by the aircraft in the EKF/NID trajectory.

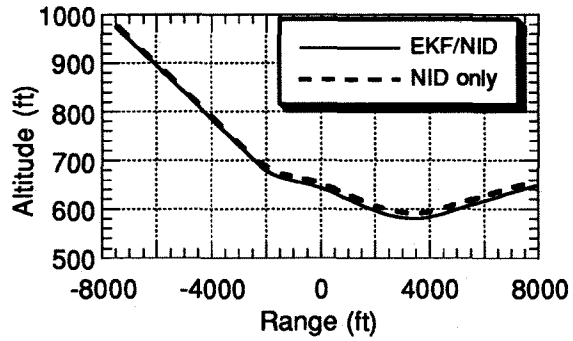

Figure 2. Altitude vs. Range.

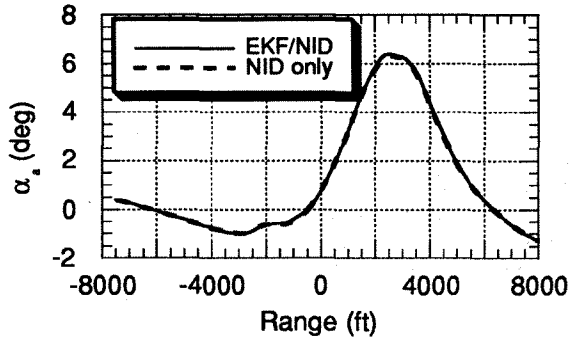

Figure 3. Angle of Attack vs. Range.

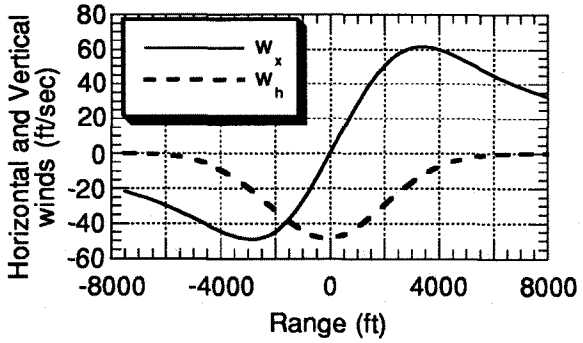

Figure 4. w_x and w_h vs. Range in the EKF/NID Trajectory.

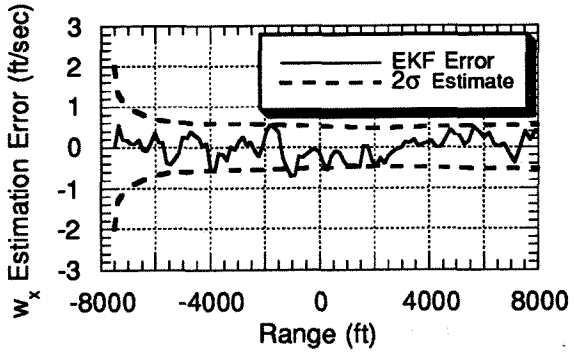

Figure 5. w_x Estimation Error in the EKF/NID Trajectory.

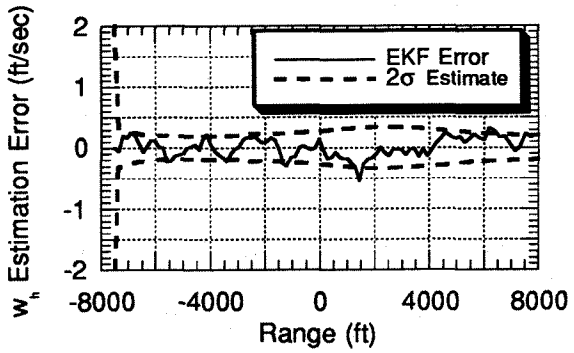

Figure 6. w_h Estimation Error in the EKF/NID Trajectory.

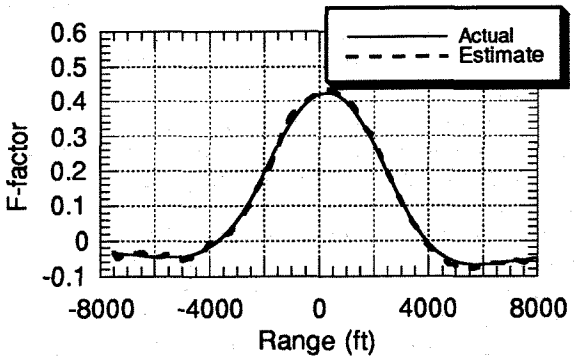

Figure 7. Actual and Estimated F-Factor in the EKF/NID Trajectory.

It is evident from Figs. 2 and 3 that the EKF/NID trajectory is qualitatively similar to the one obtained using perfect state feedback. The aborted-landing maneuver entails the use of low attack angles early in the trajectory, followed by a gradual increase that ceases near the end of the microburst core region. The EKF's ability to estimate the wind components is illustrated in Figs. 5 and 6, which present the w_x and w_h estimation errors, along with the 2σ error bounds. The actual and estimated F-Factor in the EKF/NID trajectory are shown together in Figure 7. The peak F experienced by the aircraft is approximately 0.4, indicating that this is a very severe microburst.

It is apparent that the EKF estimates the wind components accurately. The predicted 2σ error bounds are good indicators of the EKF's accuracy, implying that the actual filter performance is consistent with the expected performance. The F-Factor estimate derived from the optimal state and disturbance estimates also is quite accurate.

The results show that NID control laws can perform quite well using optimal state estimates derived from a realistic set of measurements. However, it has been assumed that the initial conditions are known exactly and that there are no modeling errors in the representation of the aircraft aerodynamics used by the EKF/NID pair. Initial condition errors result in a negligible reduction in controller-estimator performance; however, uncertainty in the aerodynamic model poses a serious problem. It has been assumed thus far that the aerodynamic model is

exact, and that any inaccuracies in calculating lift, drag, and pitching moment are due only to the errors in the state estimates themselves.

The effect of uncertainty in the aerodynamic model is examined by intentionally adding an error to the lift and drag estimates used by the EKF/NID pair. The simulation is repeated using the same microburst parameters as in Figs. 2 - 7, but now a 10% error is added to the lift and drag estimates used by both the EKF and the NID control laws. Figures 8 and 9 present altitude and angle of attack vs. range in the resultant trajectory. For comparison purposes, the response obtained using the NID control law with perfect state feedback and an exact aerodynamic model is also shown. Wind component estimation errors in the EKF/NID trajectory are shown in Figs. 10 and 11.

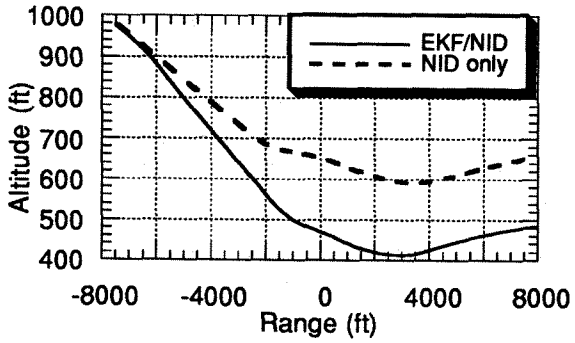

Figure 8. Altitude vs. Range – 10% Error in Lift and Drag Estimates.

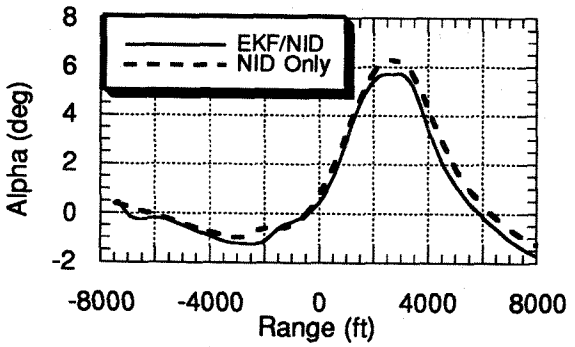

Figure 9. Angle of Attack vs. Range – 10% Error in Lift and Drag Estimates.

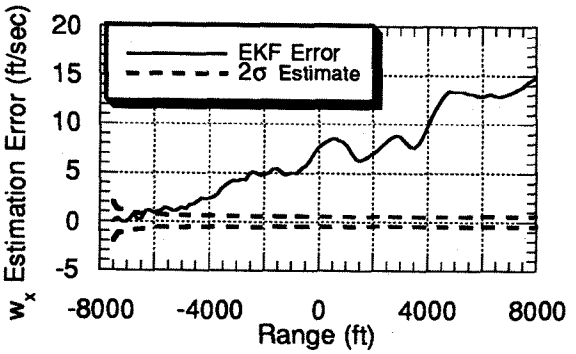

Figure 10. w_x Estimation Error in the EKF/NID Trajectory – 10% Error in Lift and Drag Estimates.

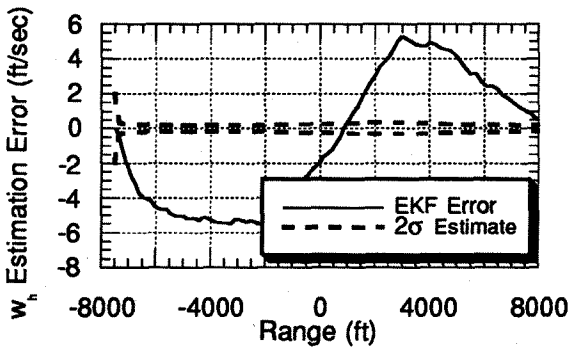

Figure 11. w_h Estimation Error in the EKF/NID Trajectory – 10% Error in Lift and Drag Estimates.

It is apparent that the modeling errors produce a dramatic departure from the nominal flight path (as defined by the NID-only trajectory). The minimum altitude in the EKF/NID trajectory is some 175 ft lower than in the NID-only trajectory. The aircraft does not track the desired approach path properly in the descent portion of the trajectory. Figures 10 and 11 show that the predicted 2σ error bounds are not good indicators of the EKF's performance. The w_x estimation error appears to grow without bound.

Uncertainty in the aerodynamic model appears to be a major stumbling block to the implementation of the EKF/NID estimator-controller pair. Since it is unlikely that an aircraft's aerodynamic model will ever be known exactly, it is necessary to devise a means of accommodating this uncertainty into the design. One such method is now discussed.

Effect of Adding Fictitious Process Noise

A simple solution for accommodating uncertainty into the design of an EKF is to add fictitious process noise $\mathbf{w}_f(t)$ [33] to the system model. In effect, uncertainty in the model is treated as a Gaussian random input. The aircraft state equations used by the EKF are modified by adding fictitious disturbance inputs to those terms that depend on lift L or drag D. The resultant model is expressed as

$$\dot{\chi} = \begin{bmatrix} \dot{\mathbf{x}}_{ac} \\ \dot{\mathbf{x}}_d \end{bmatrix} = \begin{bmatrix} \mathbf{f}(\mathbf{x}_{ac}, \mathbf{u}, \mathbf{x}_d) \\ \mathbf{F}_d \mathbf{x}_d \end{bmatrix} + \begin{bmatrix} \mathbf{w}_f \\ \mathbf{w} \end{bmatrix} \tag{51}$$

where the fictitious input $\mathbf{w}_f(t)$ is a Gaussian, zero mean random variable:

$$E\left[\mathbf{w}_f(t)\right] = \mathbf{0} \tag{52}$$

$$E\left[\mathbf{w}_f(t)\mathbf{w}_f{}^T(\tau)\right] = \mathbf{Q}_f(t)\delta(t-\tau) \tag{53}$$

The elements of $\mathbf{Q}_f$ are chosen to reflect the uncertainty in the time-rates-of-change of the components of $\mathbf{x}_{ac}$ that depend on L or D. For the simulation results that follow, $\mathbf{Q}_f$ is set to

$$\mathbf{Q}_f = \text{diag}(0, 0, 0.2, 0.05, 0.05, 0.2, 0.05, 0.05, 0, 0) \tag{54}$$

These values were chosen by trial-and-error.

The EKF/NID trajectory is now recomputed using fictitious process noise in the EKF plant model. As in the previous simulation, 10% errors are added to the lift and

drag estimates used by the EKF/NID pair. Figures 12 and 13 show the resultant altitude and angle of attack response, respectively. Once again, the profiles obtained using the NID control law with perfect state feedback and an exact model are shown for comparison purposes. Horizontal and vertical wind estimation errors in the EKF/NID flight path are shown in Figs. 14 and 15.

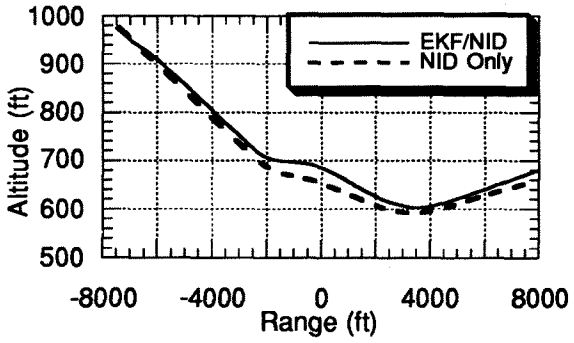

Figure 12. Altitude vs. Range – 10% Error in Lift and Drag Estimates with Fictitious Process Noise.

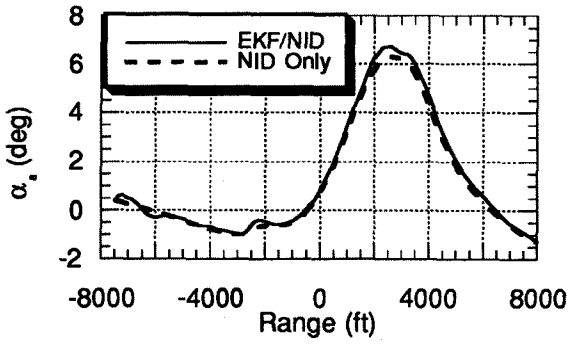

Figure 13. Angle of Attack vs. Range -- 10% Error in Lift and Drag Estimates with Fictitious Process Noise.

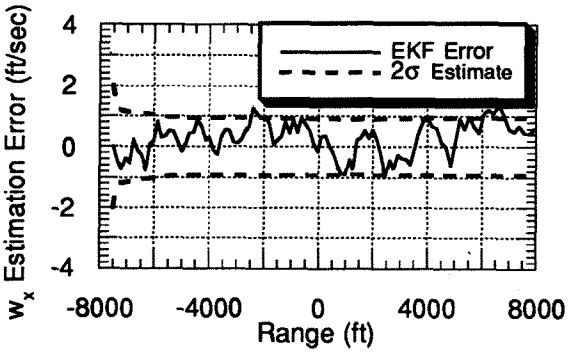

Figure 14. w_x Estimation Error in the EKF/NID Trajectory -- 10% Error in Lift and Drag Estimates with Fictitious Process Noise.

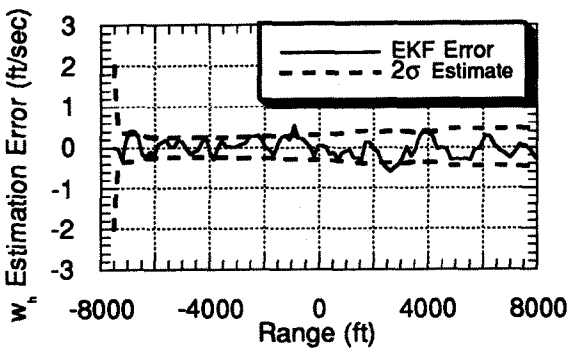

Figure 15. w_h Estimation Error in the EKF/NID Trajectory -- 10% Error in Lift and Drag Estimates with Fictitious Process Noise.

Figures 12 and 13 show that the EKF/NID altitude and angle of attack profiles with fictitious process noise are much more similar to the NID baseline than those in Figs. 8 and 9. Figures 14 and 15 demonstrate that adding the fictitious process noise restores the EKF's performance. The predicted 2σ error bounds are once again good indicators of the accuracy of the wind component estimates. The steady-state error bounds are larger in Figs. 14 and 15 than they are in Figs. 10 and 11. This may be expected, since the EKF plant model now contains uncertainty in the model itself as well as in the measurements.

The simulation results indicate that it is possible to effectively compensate for uncertainty in the plant model by adding fictitious process noise to the EKF equations. The resultant flight path is similar (but not identical) to the one obtained using perfect state feedback with an exact aerodynamic model. The EKF/NID pair function effectively a realistic set of measurements and an uncertain aerodynamic model.

Conclusions

An Extended Kalman Filter has been developed to estimate the state vector and wind disturbance inputs of a jet transport aircraft. The EKF was evaluated in concert with nonlinear control laws developed previously. Simulated flight trajectories produced using the EKF/NID pair were almost identical to those obtained using the NID control laws with perfect state feedback. The EKF produced accurate estimates of both horizontal and vertical wind inputs using a simple integral-state-model representation of the wind "system." This representation makes no assumptions about the structure of the atmospheric disturbance, and it should be able to provide accurate disturbance estimates in a variety of atmospheric conditions.

A key difficulty for applying nonlinear control and estimation techniques is uncertainty in the plant model. The use of an erroneous aerodynamic model in the EKF/NID pair led to inaccurate state estimates and poor command tracking. The introduction of fictitious process noise in the EKF equations, which treated the uncertainty as a random disturbance input, restored most of the lost

performance. This result is encouraging from a practical standpoint, because an exact aerodynamic model is not always available for control system design. Consequently, the EKF/NID control law is a good candidate for operational implementation.

References

1. Townsend, J., "Low-Altitude Wind Shear and Its Hazard to Aviation," National Academy Press, Washington, 1983.
2. Hinton, David A., "Flight Management Strategies for Escape From Microburst Encounters," NASA TM 4057, Washington D.C., 1988.
3. Bowles, Roland L., "Reducing Windshear Risk Through Airborne Systems Technology," *Presented at the 17th Congress of the Intl. Council of the Aeronautical Sciences*, Stockholm, Sweden, 1990.
4. Hinton, David A., "Piloted-Simulation Evaluation of Recovery Guidance for Microburst Wind Shear Encounters," NASA TP 2886, Washington D.C., 1989.
5. *Windshear Training Aid*, U.S. Department of Transportation, Federal Aviation Administration, Washington D.C., 1987.
6. Kupcis, Edgars A., "Manually Flown Windshear Recovery Technique," *Proc. of the 29th Conference on Decision and Control*, Honolulu, Hawaii, December 1990, pp. 758-759.
7. Miele, A., et al., "Optimal Trajectories and Guidance Trajectories for Aircraft Flight Through Windshears," *Proc. of the 29th Conference on Decision and Control*, Honolulu, Hawaii, December 1990, pp. 737-746.
8. Psiaki, M.L., and Stengel, R.F., "Analysis of Aircraft Control Strategies for Microburst Encounter," *Journal of Guidance, Control, and Dynamics*, Vol. 8, No. 5, Sept.-Oct. 1985, pp. 553-559.
9. Psiaki, Mark L., "Control of Flight Through Microburst Wind Shear Using Deterministic Trajectory Optimization," Ph.D. Thesis, Princeton University, Report No. 1787-T, 1987.
10. Psiaki, M.L., and Stengel, R.F., "Optimal Aircraft Performance During Microburst Encounter," *Journal of Guidance, Control, and Dynamics*, Vol. 14, No. 2, March-April 1991, pp. 440-446.
11. Zhao, Y., and Bryson, A.E., "Optimal Paths Through Downbursts," *Journal of Guidance, Control, and Dynamics*, Vol. 13, No. 5, Sept.-Oct. 1990, pp. 813-818.
12. Mulgund, S.S., and Stengel, R.F., "Target Pitch Angle for the Microburst Escape Maneuver," *Journal of Aircraft*, Vol. 30, No. 6, Nov. - Dec. 1993, pp. 826 - 825.
13. Mulgund, S.S., and Stengel, R.F., "Optimal Recovery from Microburst Wind Shear," *Journal of Guidance, Control, and Dynamics*, Vol. 16, No. 6, Nov. - Dec. 1993, pp. 1010- 1017.
14. Zhao, Y., and Bryson, A.E., "Control of an Aircraft in Downbursts," *Journal of Guidance, Control, and Dynamics*, Vol.13, No.5, Sept.-Oct. 1990, p. 819.
15. Miele, A., et al., "Guidance Strategies for Near-Optimum Takeoff Performance in Wind Shear," *Journal of Optimization Theory and Applications*, Vol, 50, No. 1, July 1986.
16. Miele, A., et al., "Optimization and Gamma/Theta Guidance of Flight Trajectories in a Windshear," *Presented at the 15th ICAS Congress*, London, Sept. 1986.
17. Mulgund, S.S. and Stengel, R.F., "Aircraft Flight Control in Wind Shear Using Partial Dynamic Inversion," *Proceedings of the 1993 American Control Conference*, San Francisco, June 1993.
18. Lane, Stephen, and Stengel, R.F., "Flight Control Using Nonlinear Inverse Dynamics," *Automatica*, Vol. 24, No. 4, pp. 471-483, 1988.
19. Menon, P.K.A., et al, "Nonlinear Flight Test Controllers for Aircraft," *Journal of Guidance*, Vol. 10, No. 1, Jan-Feb 1987.
20. Menon, P.K.A., et al, "A Two-Time-Scale Autopilot for High Performance Aircraft," *Presented at the 1991 AIAA Guidance, Navigation, and Control Conference*, New Orleans, Aug. 1991.
21. Meyer, G., and Cicolani, L., "Application of Nonlinear System Inverses to Automatic Flight Control Designs -- System Concepts and Flight Evaluations", in *Theory and Application of Optimal Control in Aerospace Systems*, AGARD -- AG251, pp. 10.1-10.29.
22. Hauser, J., Sastry, S., and Meyer, G., "Nonlinear Control Design for Slightly Non-minimum Phase Systems: Application to V/STOL Aircraft," *Presented at the IFAC Conference NOLCOS '89*, Capri, Italy, June 1989.
23. Elgersma, M., and Morton, B., "Partial Inversion of Noninvertible Nonlinear Aircraft Models," Honeywell Systems Research Center, Minneapolis, MN, Aug. 1989.
24. Frost, W., and Bowles, R., "Wind Shear Terms in the Equations of Aircraft Motion," *J. of Aircraft*, Vol.21, No.11, Nov.1984, pp.866-872.
25. Stengel, R.F., *Course Notes for MAE 566: Aircraft Dynamics*, Princeton University, Princeton, NJ, Jan. 1990.
26. Oseguera, R.M., and Bowles, R.L., "A Simple, Analytic 3-Dimensional Downburst Model based on Boundary Layer Stagnation Flow," NASA TM 100632, Washington D.C., 1988.
27. Singh, S.N., and Rugh, W.J., "Decoupling in a Class of Nonlinear Systems by State Feedback," *ASME J. Dyn. Syst. Meas. Cont.*, Series G, Vol. 94, Dec. 1972, pp. 323-329.
28. Isidori, A., *Nonlinear Control Systems*, Springer-Verlag, Berlin, 1989.
29. Stengel, R.F., "Toward Intelligent Flight Control," *Presented at the NATO-AGARD Workshop on Stability in Aerospace Systems*, Toulouse, France, June 23-26, 1992.
30. Chow, J. and Kokotovic, P., "Two-Time-Scale Feedback Design of a Class of Nonlinear Systems," *IEEE Transactions on Automatic Control*, Vol. AC-23, No. 3, June 1978.
31. Etkin, B., *Dynamics of Atmospheric Flight*, Wiley, New York, 1972.
32. Psiaki, M., and Park, K., "Thrust Laws for Microburst Wind Shear Penetration," Journal of Guidance, Control, and Dynamics, Vol. 15, No. 4, July-Aug. 1992.
33. Gelb, A., ed., *Applied Optimal Estimation*, MIT Press, Cambridge, MA, 1974.
34. Hansen, R., "Boeing Windshear Systems," AIAA Paper 87-2342, 1987.
35. Johnson, B., "Sensing Windshear," *Sensors*, March 1986.
36. Oseguera, R., Bowles, R., and Robinson, P., "Airborne In Situ Computation of the Wind Shear Hazard Index," AIAA Paper 92-0291, *Presented at the 30th Aerospace Sciences Meeting*, Reno, NV, Jan 6-9, 1992.
37. Bossi, J., and Bryson, A.E., "Disturbance Estimation for a STOL Transport During Landing," AIAA Paper 81-0018, *Presented at the 19th Aerospace Sciences Meeting*, St. Louis, MO, Jan. 12-15, 1981.